INFLUENCE OF PRECIPITATION ON RECRYSTALLIZATION AND TEXTURE DEVELOPMENT IN AN Al-1%Mn-0.5%Mg ALLOY

O. Daaland[1] and E. Nes[2]
1. Hydro Aluminium a.s, R & D Centre, Karmøy, N-4265 Håvik, Norway
2. Norwegian Institute of Technology, Department of Metallurgy, 7034 Trondheim, Norway

Abstract

In the present study a detailed investigation of the recrystallization texture development has been performed in an AlMnMg alloy, which was hot rolled followed by cold rolling and subsequent annealing treatment. A characteristic aspect during annealing at low temperature is a 'coarse grain' surface layer with a strong texture consisting of a major {001}<310> and minor {110}<111> and {001}<100> components. All these components are characterized by a 40°<111> orientation relationship towards major rolling texture components, the two former towards the copper component ({112}<111>) and the latter towards the S-component ({123}<412>). By using the EBSP-technique for identification of the individual grain orientations, the growth of the surface grains has been monitored in detail. The 40°<111> type grains are shown to grow significantly faster than the random oriented grains and they consume the latter making them "island" grains. It is important that the softening reaction at low temperature annealing is accompanied by a precipitation reaction occuring concurrently with recrystallization. The detrimental effect of precipitation on the nucleation and growth characteristics of different texture components is discussed. Furthermore, the effect of different growth rates on the structure and texture development has been illustrated by means of computer simulations of the recrystallization reaction.

Introduction

The origin of recrystallization texture formation has been a subject of debate for many years, and has been ascribed to both 'oriented nucleation' and 'oriented growth' interpretations [1]. The basic concept of oriented growth is that grains with a special orientation relationship to the deformed matrix will have a growth advantage compared with grains of random orientation. In fcc-metals grains with a 40°<111> orientation relationship seem to be of this special character. However, experimentally there have been few attempts in the past to directly measure and compare the growth rate of 40°<111> components/grains to that of grains belonging to other texture components, in order to prove a possible oriented growth effect. In addition, some recent investigations [2] have suggested that that the 40°<111> orientation relationship seems to be related to nucleation rather than to growth. The main objective of the present work has been to study in detail the growth of strong 40°<111> components during annealing. Special focus has been directed towards the influence of precipitates on the recrystallization texture development, which is a major problem during processing of industrial/commercial alloys.

Experimental

A commercial AlMnMg-alloy with the following chemical composition has been investigated: 1.02 wt.% Mn, 0.51 wt.% Mg, 0.16 wt.% Si, 0.4 wt.% Fe. The alloy was received as 20mm thick hot rolled slab. Further processing of the material was performed by cold rolling in a laboratory rolling mill to a strain of ε=3,5. Annealing treatment was finally carried out in a salt bath at 300°C and 450°C, respectively. Macroscopic textures was determined from X-ray pole figures, and the results were presented as Orientation Distribution Functions (ODFs). The growth of recrystallized grains was followed using the EBSP-technique on a series of partly recrystallized samples. In order to link individual orientations to the microstructure, electron channelling contrast micrographs of the investigated areas were recorded. To quantify the EBSP-data the grains were classified into several groups or ideal orientations {hkl}<uvw>, corresponding to the main recrystallization textures observed, i.e. ND rotated cube {100}<310>, P {110}<111> and cube {100}<001> grains. If the registered grain orientation was within ~15° from one of the above defined ideal components it was classified as belonging to that specific component. Grains with other orientations, not being among the main recrystallization texture components {hkl}<uvw> were designated as being part of the random component. For each annealing condition on average 200 grain were analysed and their size (grain area) measured from channelling contrast micrographs using a computerised image analyser (Kontron Videoplan).

Results

Global texture development As shown by the ODF in Fig. 1(a), a characteristic feature in the hot rolled slab is a strong {001}<110> shear texture (45° ND-rotated cube) in the surface region of the sheet, penetrating to depths of 1/3 of the sheet thickness.

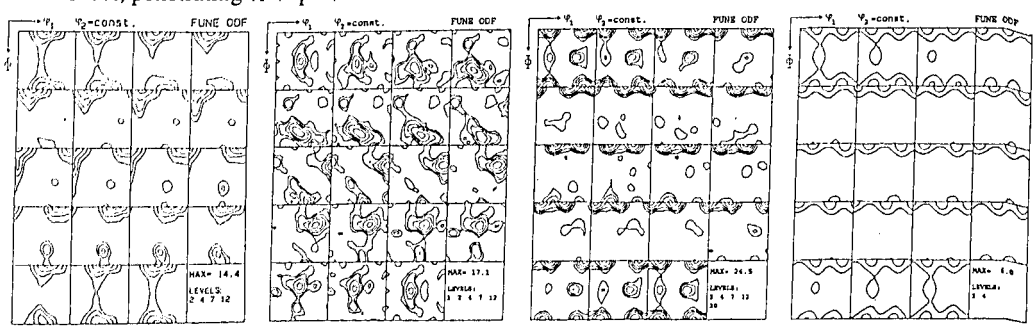

(a) (b) (c) (d)

Figure 1. ODFs, surface region of the sheet: (a) hot rolled slab, (b) cold rolled to strain, ε = 3.5, (c) cold rolled + annealed at 300°C, (d) cold rolled + annealed at 450°C.

The initial shear texture (Fig. 1a) is found to be unstable during plane strain deformation and cold rolling therefore results in the development of a ß-fibre (Fig. 1b) with intensities of 17, 14 and 8 x random at the Cu, S and Bs positions, respectively. Subsequent flash annealing treatment of the alloy performed at 300°C, resulted in a 'coarse-grain' and inhomogeneous structure in the surface region of the sheet. This surface-grain-size-effect also involves a texture aspect. As can be seen from Fig. 1c the surface grain structure is associated with a characteristic texture consisting of a

major ND rotated cube component, {001}<310>, and minor components of P, {110}<111>, and cube {001}<100>. The strong components observed in this case are of special interest in the 'oriented growth'/'oriented nucleation' context since they are associated with a 40°<111> orientation relationship to components in the rolling texture. From an 'oriented growth'-point of view, however, it is rather strange that annealing of the material at 450°C, results in a much weaker texture (Fig. 1d) and a fine grain size.

Growth of Recrystallized Grains The growth of recrystallized grains in the surface region of the sheet has been studied in detail during annealing at 300°C. The grain size measurements are presented in two different ways in Fig. 2 - the average grain diameter (D) vs. annealing time and the largest grain (D_{max}) vs. annealing time. From the average grain size vs. annealing time-plot (Fig. 2a) it is obvious that a strong relationship exists between the size of the grain and its orientation. Grains of different orientations grow at different rates, the ND rotated cube, P and cube grains growing significantly faster than the random grains. The grains belonging to the random category seem in fact to stop growing completely after reaching a size of approximately 7 - 8 μm in average diameter. During the rest of the recrystallization period the growth of these random-grains (presumably nucleated from particles by means of PSN) are obviously hindered and they are often engulfed by larger recrystallized grains becoming "island" grains.

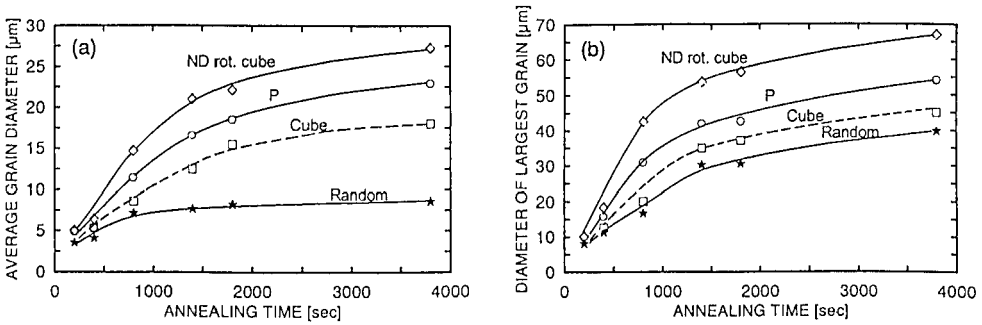

Figure 2. Evolution of different grain orientations in the surface region of the sheet during annealing at 300°C, (a) Average grain diameter vs. annealing time and (b) Largest grain diameter vs. annealing time.

Table 1: Volume fraction and number of grains for the different texture components

Annealing time		200	400	800	1400	1800	4000
Volume fraction (%)	ND rotated cube	1	3	10	27	34	48
	P	-	1	5	11	12	26
	Cube	-	1	1	4	5	17
	Random	2	4	6	10	10	9
	Total	3	9	22	52	61	100
Number of grains per unit volume ($/m^3$)	ND rotated cube	$2 \cdot 10^{14}$	$2 \cdot 10^{14}$	$6 \cdot 10^{13}$	$6 \cdot 10^{13}$	$6 \cdot 10^{13}$	$5 \cdot 10^{13}$
	P	-	$2 \cdot 10^{14}$	$6 \cdot 10^{13}$	$5 \cdot 10^{13}$	$4 \cdot 10^{13}$	$4 \cdot 10^{13}$
	Cube	-	$6 \cdot 10^{13}$	$3 \cdot 10^{13}$	$4 \cdot 10^{13}$	$3 \cdot 10^{13}$	$3 \cdot 10^{13}$
	Random	$9 \cdot 10^{14}$	$1 \cdot 10^{15}$	$3 \cdot 10^{14}$	$4 \cdot 10^{14}$	$3 \cdot 10^{14}$	$3 \cdot 10^{14}$

In Table 1, all the important transformation data obtained from the EBSP-investigation are listed. By assuming random distribution of sites and spherical grains, the measured area fraction of the texture components is equal to the volume fraction. The table also includes the approximate nuclei/grain-density, calculated assuming the growing grains to be spherical. A rather curious observation is the drastic reduction in the number of nuclei in the early stages of recrystallization. A significant drop by a factor of approximately 3 is observed for all the texture components between 400 and 800 seconds of annealing. On further annealing the nuclei/grain densities remain reasonably constant.

Discussion

An obvious interpretation of the results, when considering only the transformation curves in Fig. 2, seems to be a strong oriented growth effect, i.e. the 40°<111> oriented grain boundaries have a higher mobility than boundaries between grains of random orientation. However, taking a closer look at the experimental observations, such a boundary mobility interpretation does not appear convincing. A main deficiency is the fact that the higher mobility of the ND rotated cube, P and cube grains seems to be operative only in the early stages of recrystallization. As shown in Fig. 2b for the evolution of the largest grain, the 40°<111> components are growing faster only in the first 20-30% of recrystallization. In a classical oriented growth situation the 40°<111> component should have continued to grow at a higher rate than the random component, during the entire transformation. However, this is not observed. Another point which also disfavours a classical oriented growth interpretation is connected to the observation of a much weaker recrystallization texture when the material is annealed at a higher temperature. The growth reaction at 450°C has not been investigated, due to the very short annealing times required to produce partly recrystallized structures. However, measurements of grain sizes have been performed on a fully recrystallized sample annealed at 450°C and the 40°<111>-grains (ND rotated cube and P) are in this case found to be of the same size as the random grains. This of course indicates that the PSN-grains in this case are able to grow as rapidly as the others. It is to be noted that simple calculation shows that the nuclei/grain-density (or the number of activated sites) is the same during annealing at 300° and 450° (of the order 10^{15} m^{-3}).

Influence of concurrent precipitation From the above discussion, it follows that the strong growth selection effect during low temperature annealing must be due to other reasons than a classical oriented growth effect. It is known that the cast ingot was preheat treated in a way leading to retainment of a large amount of elements in solid solution before the start of hot rolling. Hot rolling was subsequently performed with a relatively rapidly falling temperature, and subsequent cold rolling and annealing at a low temperature resulted in precipitation of Fe-, Mn-bearing phases occurring concomitantly with recrystallization. Such a reaction has been confirmed by conductivity measurements (Fig. 3), and it seems reasonable that the observed drop in the number of activated sites can be accounted for by such a heavy precipitation. All components are therefore affected by the precipitates, but the PSN grains are obviously the ones most severely affected. A reasonable hypothesis describing this phenomenon may be given by assuming the following :

(1) Nucleation and growth of recrystallization can be described as a competition between PSN and nucleation from banded features within the deformation microstructure.

(2) Nuclei of size equal to (or larger than) the critical Gibbs-Thompson diameter for nucleation are expected to be present inside these band-heterogeneities of ND-rotated cube, P and cube orientation, in the as-deformed condition.

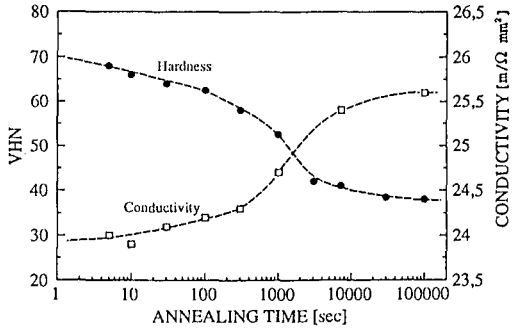

Figure 3. Electrical conductivity as a function of annealing time.

The occurrence of such banded features (of the cube orientation) has been documented in detail by Daaland [3] in a similar alloy. It is furthermore emphasised that peaks at the ND rotated cube and P position are found in the ODF of the as-cold rolled structure (Fig. 1b), an observation which proves that these orientations are indeed present in significant proportions in the as-deformed condition. The nuclei of ND rotated cube, P and cube orientation, which have reached the critical Gibbs-Thompson diameter, is assumed to start growing at time t=0 simultaneously with the start of precipitation. This behaviour contrasts with the nucleation and growth of the PSN-grains, which invariably develop from much smaller cells, and requires subgrain growth and recrystallization out of the deformation zone, before reaching the critical Gibbs-Thompson diameter. During the time required to consume the deformation zone sufficient precipitation will take place, and a large amount of the PSN-nuclei therefore will have great difficulty in growing out of the zone. Such a simple hypothesis has been treated in detail by Daaland [3] who showed that the total Zener-drag pressure is of the same order as the driving pressure for recrystallization, resulting in an effective driving pressure being zero. This means that unless a new PSN-grain has consumed the deformation zone, before impingement on the precipitated phase, further growth of the nuclei will be very difficult. Most of the PSN-nuclei therefore will stay small and get surrounded or consumed by the more rapidly growing ND rotated cube, P or cube grains. This picture is consistent with the experimental observation of "island" grains. The grain size distributions for fully recrystallized structures are shown in Fig. 4. Annealing at low temperature results in an extremely broad size distribution. High temperature annealing, on the other hand, results in a typical 'log normal' distribution.

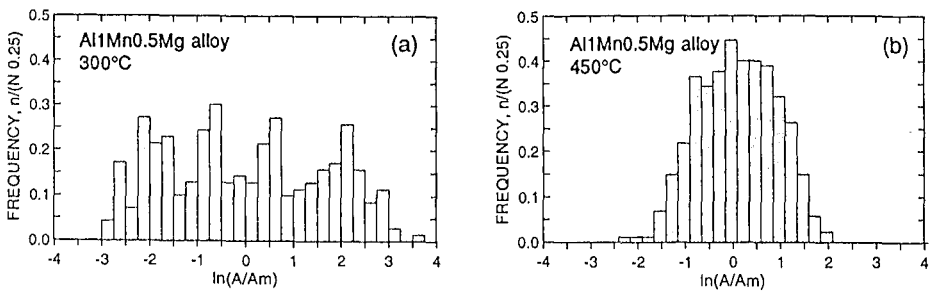

Figure 4. Experimental grain size distribution, (a) annealing at 300°C, (b) annealing at 450°C

Computer simulations of recrystallization To gain some more insight into the recrystallization reaction, computer simulations have been performed. For details about the computer model used, see reference [3, 4, 5, 6]. The main purpose was to investigate the effect of grains growing at different rates, on the final grain size distribution.

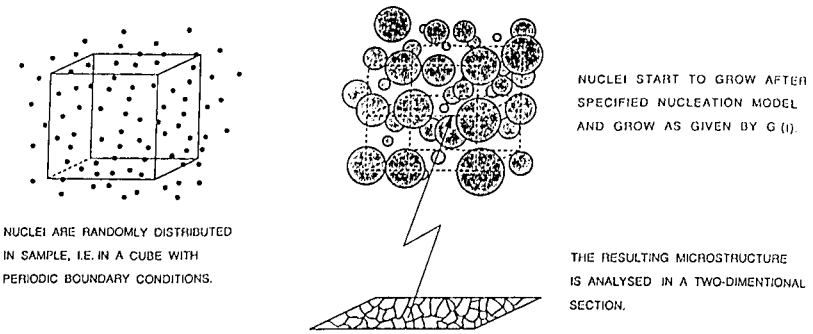

Figure 5. Principles of the computer simulation procedure

In the present work the model has been modified by introducing a non-uniformity with respect to how the grains grow, allowing the textural aspect of recrystallization to be studied. Nuclei were distributed between four different classes according to the nuclei/grain-density numbers calculated for each classified texture component (see Table 1). As a first approach (Case I), a specific growth rate was then assigned to each class, corresponding to the difference in initial growth rate observed experimentally, i.e from studying the growth of the largest grain, Fig. 2b. The grains were subsequently allowed to grow isotropically at constant rates until impingement. In addition to using constant but different growth rates for each class, simulations have also been performed in which each class were associated with a decreasing growth rate different from the others (Case IIA). A further refinement of the simulation procedure (Case IIB) has been included by taking into account the experimentally observed drop in the number of grains (or nuclei) during the transformation. Using the same condition for growth as in Case IIA, this effect was achieved in the simulation by physically stopping 2/3 of the grains of each class after a total transformation of 10%. All simulations were performed using site saturation nucleation kinetics (i.e. all nuclei activated at time, t=0), and the nuclei were randomly distributed in space.

The simulated and experimental results, in terms of average grain sizes in the fully recrystallized state, are listed in Table 2. A general underestimation of the experimentally observed grain size is obtained Case I. Somewhat larger grain sizes are predicted in the simulation Case IIA, however, the average grain size for the different classes are still too small compared with the experimental observations. A reasonably good fit is observed in the last simulation approach, Case IIB. Except for the slowest growing random component, the experimental and simulated results for the other components are well in line.

The grain size distributions obtained in the computer simulations are shown in Fig. 6. Using constant but different growth rates (Case I) results in a significant broadening of the size distribution, Fig. 6a. Note that when the size distribution of each separate class is plotted, site saturation distributions are obtained. When different classes are combined in a simulation their individual site saturation peaks will be superimposed resulting in several peaks in the size

distribution. The use of decreasing growth rates further broadens the distribution, as shown in Fig. 6b and c. However, compared with the experimental results (Fig. 4(d)) all the simulated distributions are somewhat more narrow. This indicates that the recrystallization process is more complex than assumed by the simulation model. It is noted, however, that Case IIB comes close to the experimental observations.

Table 2: Experimental and simulated grain sizes [μm], fully transformed state.

		Computer sim.		
Texture component	EBSP	Case I	Case II	Case III
ND rotated cube	27	19	22	27
P	23	16	18	22
Cube	18	15	15	17
Random	9	6	6	6

The simulated results for the fraction of recrystallized material as a function of annealing time, is shown in Fig. 7. The results have been plotted in the classical way for a JMAK-interpretation, i.e. logln[1/1-X(t)] versus log t. For the simulation Case I, a least square fit to a straight line yields a slope of 3 in accordance with the original site saturation case. This is not surprising since the simulation in Case I in kinetic terms is equivalent to simulations using only one component. However, when decreasing growth rates are included in the simulation the n-value is reduced to 2.5 and 1.8 for Case IIA and Case IIB, respectively. The latter value, which takes into account the concurrent precipitation reaction in the early stages of recrystallization, is in reasonable agreement with the experimentally observed value of 1.6.

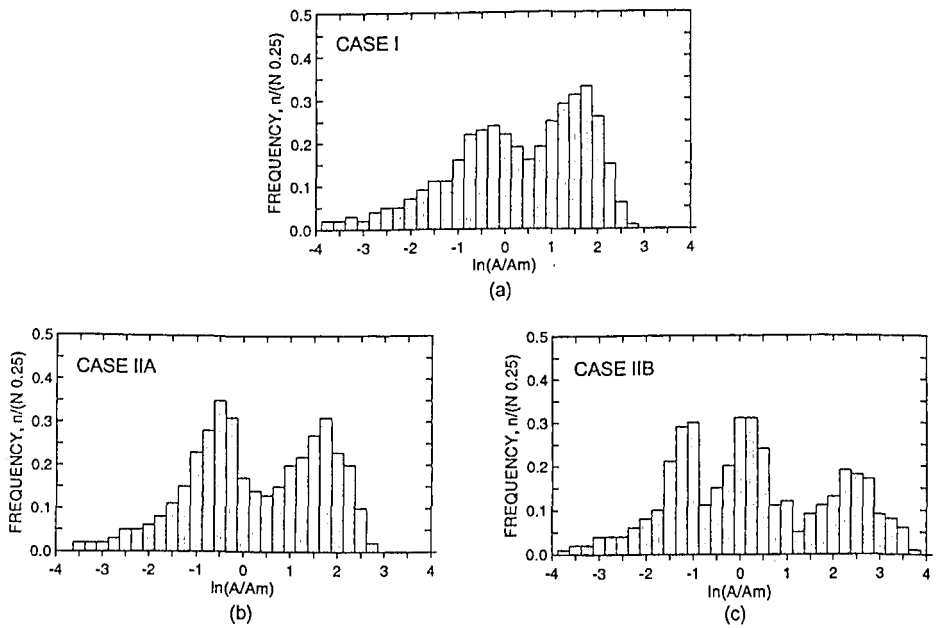

Figure 6. Grain size distributions obtained from simulation (a) Case I, (b) Case IIA, (c) Case IIB. (Experimental distribution for the Al-Mn-Mg alloy annealed at 300°C is shown in 4(d)).

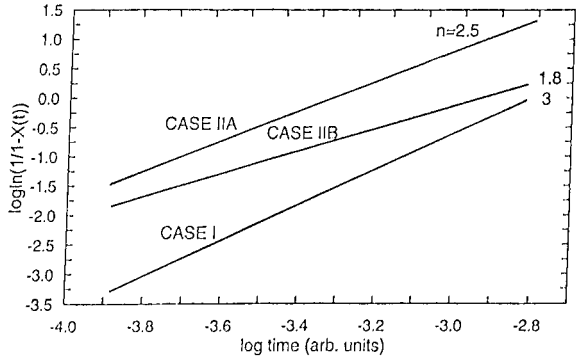

Figure 7. Transformation kinetics (JMAK-plot) for the cases investigated by means of computer simulation.

Conclusions

- The more rapid growth of the ND rotated cube, P and cube grains at low temperature annealing of the Al1Mn0.5Mg alloy is due to a precipitation-induced effect. The higher growth rate of the 40°<111> components reflects that these grains have a much shorter "incubation time" for nucleation than the random category, and accordingly become less affected by the concurrent precipitation occurring at low annealing temperatures.

- The computer model which has been employed is not fully capable of simulating the recrystallization process in the present alloy. However, computer simulation using four components improves the simulation prediction, compared to a more simple modelling approach in which all grains are considered to behave alike (i.e. using only one growth rate). A size distribution being much broader in combination with a JMAK-exponent (Case IIB) being close to the experimentally observed value, indicates that the model has important elements in it which are closer to a correct description of the recrystallization reaction. It is expected that the experimental situation corresponds to a dispersion of growth rates within each class, instead of four distinct growth rates used in the present simulations.

References

1. Doherty, R. et al., ICOTOM 8, Warrendale Pa, 563 (1988).
2. Hjelen, J. Ørsund, R. and Nes, E., Acta. Met., 39, 1377 (1991).
3. Daaland, O., PhD thesis, Norwegian Institute of Technology, University of Trondheim (1993).
4. Sætre, T. O., Hunderi, O. and Nes, E., Acta. Met., 34, 981 (1986).
5. Marthinsen, K., Lohne, O. and Nes, E., Acta. Met., 37, 135 (1989).
6. Furu, T., Marthinsen, K. and Nes, E., Mat. Sci. Tech., 6, 1093 (1990).